

DISCLAIMER

This document was prepared as an account of work sponsored by an agency of the United States Government. Neither the United States Government nor any agency thereof, nor any of their employees, makes any warranty, express or implied, or assumes any legal liability or responsibility for the accuracy, completeness, or usefulness of any information, apparatus, product, or process disclosed, or represents that its use would not infringe privately owned rights. Reference herein to any specific commercial product, process, or service by trade name, trademark, manufacturer, or otherwise does not necessarily constitute or imply its endorsement, recommendation, or favoring by the United States Government or any agency thereof. The views and opinions of authors expressed herein do not necessarily state or reflect those of the United States Government or any agency thereof.

BNL 31389

Conf-820814-15

NUCLEAR REACTORS USING FINE-PARTICULATE FUEL FOR PRIMARY POWER IN SPACE*

BNL-31389

T.E. Botts, J.R. Powell, J.L. Usher, and F.L. Horn

DE02 016746

Brookhaven National Laboratory
Upton, New York 11973

Abstract

Large future power requirements in space, include power beaming to earth, airplanes, and solar-powered satellites in eclipse; industrial processing; and space colonies. The Rotating Bed Nuclear Reactor (RBR) and Fixed Bed Reactor (FBR) are multi-megawatt power systems which are light, compact and suited to operation in space. Both are cavity reactors, with an annular fuel region (e.g. a bed of 500 μ HTGR fuel particulates made of UC with ceramic coating) surrounded by a reflector that moderates fast neutrons from the ^{235}U fuel. A porous metal drum holds the fuel. In the RBR, rotation of the drum allows the particulate fuel bed to fluidize as cooling gas passes through. In the FBR, an inner porous carbon drum holds the packed fuel bed, which is not fluidized. The RBR and FBR have many important features for space nuclear power: very high power density (up to thousands of MW(th)/m³ of fuel); very small size and weight; excellent thermal shock and fatigue resistance; short start/stop times (sec); high gas outlet temperatures (to 3000 K), good neutron economy, low critical mass; and simple/reliable construction.

INTRODUCTION

As man goes into space, he takes with him requirements for substantial quantities of power and energy. This power can be produced in space and beamed to earth where it can be used at remote ground sites, or to power airplanes. Applications in space include high-powered radar, beam power for solar-powered satellites in eclipse, and to provide prime power for space-based industries and manned colonies.

What stands as a major impediment to the availability of large power supplies in space is the need for fundamentally new technology which can meet such loads simply with a minimum of material involved. Higher specific power (power/unit throw weight) for a space power station relaxes energy requirements to achieve orbit and can possibly reduce the busbar cost of space power. Toward this goal of very high specific power for space-based power stations, two nuclear reactor concepts have been proposed at Brookhaven National Laboratory.

The first of these reactors is the RBR (Fig. 1). The RBR is an externally-moderated cavity reactor. The core is a rotating fluidized bed of

UC/Zr coated particles very similar to BISO (Fig. 2.b) particles currently used in high-temperature, gas-cooled reactors (HTGR). Coolant gas enters the bed through a porous metal frit after cooling the reflector/moderator and the cavity exit nozzle. This configuration allows the heated coolant, which can be as hot as 3000 K, to come into contact with an absolute minimum amount of structural material.

The FBR (Fig. 3) is neutronically similar to the RBR. Fuel is held in place with an inner porous frit, rather than a rotationally induced field. Maximum outlet temperature from this reactor is lower than with a RBR, on the order of 2500 K.

Both reactors are controlled via rotating drums in the outer reflector/moderator region. The reactors are thermalized and very sluggish in response to reactivity insertions, so that control is simple and safe. Because of the small size (~600 to 800 μ) of the fuel particles, the fuel is highly insensitive to thermal shock. TRISO particles have historically shown high fission product retention (99.99%) up to very high burnup (>50%), and operation in a FBR or RBR should do nothing to degrade this performance. It is possible, from the point of view of neutronics, to bring the reactor from 0.1% power to full power in a few sec. Thus, fluctuations in load can easily be followed.

For minimum throw weight and simplicity, dynamic Brayton power conversion appears best suited. Total power and energy requirement determine the optimum energy conversion system. Low total energy requirements tend to favor open-cycle with working fluid vented to space. Low power requirements favor a turbine and alternator while magnetohydrodynamic (MHD) energy conversion systems are smaller and lighter at high power levels.

Algorithms for total system weight and output power, define open/closed and turbo-alternator/MHD regions of operation. Hydrogen, stored as a cryogenic liquid, is used for open-cycle operation due to its low molecular weight. Closed-cycle operation favors He as the working fluid due to its excellent heat transfer characteristics. Brayton cycles using dissociating gases (e.g., N₂O₄) are also being considered for closed-cycle operation, and preliminary results are quite encouraging. Such a working fluid has excellent heat transfer characteristics and offers the possibility of 40 to 50% efficient electrical conversion.

MASTER

*Research carried out under the auspices of the U.S. Dept. of Energy.

Both of these characteristics lead to lighter space-based power systems. Closed-cycle operation in space requires radiative heat injection. Gas-filled tubes, heat pipes, dust, and Liquid Droplets Radiators (LDR) are being considered. Tube and heat pipe radiators have specific powers on the order of 1 kW/kg for a reject temperature of 600 K. The LDR should have a specific power of around 40 kW/kg at 600 K. Multi-megawatt closed-cycle space power stations will require such types of heat rejection if they are to be put into orbit using the shuttle or shuttle-derived heavy launch vehicle.

Power Conversion Cycles

Open- and closed-Brayton cycles using either turbogenerators or MHD channel for electrical power generation, have been considered. For closed cycles, regeneration would be used only with finned tube and heat pipe radiators. A recuperator can reduce the reject power and radiator weight by ~15%. Nonregenerative Brayton cycles are preferred when lightweight LDR are used.

Due to the fourth power temperature relationship for radiated power, reject temperatures in space are higher than for a ground-based power plant. Table 1 illustrates the efficiency of a range of regenerative and nonregenerative Brayton cycles using turbines and compressors with representative efficiencies. Lower efficiency implies a larger turbine, compressor, heat exchangers, and piping. With a LDR, reject temperature can be as low as 500 to 600 K with the radiator representing only ~15% of total system weight. Benefits of lower reject temperature and higher efficiency are very important. Power stations using finned tube or heat pipe radiators must operate at higher temperatures to achieve feasible throw weights. For a reject temperature of 700 - 900 K, fixed radiators are 85 to 95% of the total power system weight. At 100 MW(s), the specific power of an optimized FBR-based power station using a conventional radiator is roughly 0.15 kW/kg and using a LDR, the specific power is 5.0 kW/kg.

For closed-cycle turbine-based FBR systems, radiator development offers the opportunity for significant improvements in specific power. High temperature turbine blades and light-weight casings are next most important.

At power levels >100 MW(s), MHD power conversion become attractive. Specific powers of 25 to 50 kW/kg appear achievable. Table 2 illustrates two designs of MHD channels. Two output temperatures represent the peak output temperatures of the FBR and RBR. Clearly, the higher temperature yields a more compact, efficient unit. Such a system, operating in an open-cycle could provide prime power for heavy lift orbital transfer vehicle using electric thrusters. In the closed-cycle mode, bottoming turbine fairly high overall efficiencies and lower reject temperatures than possible with straight MHD.

Scaling Relationships

Weight and volume algorithms have been devised for RBR and FBR space power systems at the component level. A computer code sizes the components of a closed-loop space-power station using either a turbo-alternator or MHD channel for power conversion. Open-cycle power plants are to be included in future analyses. Table 3 shows some weight algorithms used in the analysis.

Turbine and compressor weights, volumes, and performance characteristics are from published projections (1-4). Weight reduction is possible for turbines and compressors by matching the alternator to the turbine speed and eliminating the gear box. For the present time, only the second area has been considered. (The superconducting generator, being built at Wright-Aeronautical Laboratories (5), is coupled directly to the turbine, and provides a significant weight savings. The WP machine is not continuously rated, however, and would be somewhat heavier for cw operations.)

The MHD channel chosen for these design studies is a channel with a standoff wall of BN with ZrO_2 electrodes and a Mo alloy case. Cryogenic AL magnets are used. A superconducting magnet might be lighter, but introduces the problems of quenches, etc. This is the same reason why alternators using rare earth magnets was chosen over superconducting units, which offer potentially superior performance, for turbine power conversion systems.

Piping is all Ti alloy, with stand-off insulation where very high temperatures are present. Maximum allowable hoop stress is ~300 MPa.

Recuperators and heat exchangers to radiators, where needed, are also made of Ti alloy. These component weights are important and detailed computer generated point designs of the entire He loop were used to obtain their size and weight over a range of output power levels.

Three radiators were considered in the initial design phase: heat pipes (6), tubular (7), and liquid droplet (7). The tubular radiator does away with one heat exchanger, making it somewhat lighter than the heat pipe radiator. Both the heat pipe and tubular radiator are more massive than the LDR, which also allows lower reject temperatures. For this reason, only the LDR is presented here. At lower power levels, where the radiator is a smaller fraction of the total weight of a power station, all three means of heat rejection offer similar system weights. For ease of evaluating the manner in which RBR/FBR power stations scale with power, only LDR are presented. For temperatures above 400 K, Li is the working medium, and at lower temperatures, silicone vacuum oils are used. Choices of working fluid is mentioned, significantly impacting radiator weight.

The reactor, either RBR or FBR, has a minimum size due to criticality considerations, and this size does not vary much over the power ranges considered. The primary variation of reactor weight is due to the increased pressure vessel thickness at higher powers. This results from the need for a higher He pressure in the fuel bed as the power density increases.

Shield weight and volume are only slightly dependent on power level. They are primarily driven by reactor size, shielding materials, and the required level of shielding. A combination of LiH and W has been selected as the shielding material. Shield weight and volume will be strongly a function of application. For this reason, when comparing power cycles, the shield weight is not shown.

Figure 4 illustrates the total computed weight of a space power station. Both open-cycle, with varying lifetimes, and closed-cycle operations are illustrated. Below 100 MW(e), a FBR is used and at higher powers a RBR is used. In all cases, one or more turbo-alternators are used for power conversion. Introducing MHD power conversion above 100 MW(e) would decrease slightly the marginal weight of the system at higher power levels. Nevertheless, at much over 100 MW(e), the power station cannot be placed in low earth orbit using the space shuttle. At low power levels, below ~10 MW(e), the fixed weight associated with critical reactor dimensions places a lower limit on power system weight. Table 5 illustrates the variation in specific power with output power level as well as for closed-cycle operation.

Figure 5 demonstrates the weight trade between closed-cycle operation using hydrogen as a working fluid. Both systems modeled use a 100 MW(e) output FBR and drive a turbo-alternator. A Li LDR is used for heat rejection in closed-cycle operation. If the same trade is carried out, using a tubular radiator, the trade-off time increases to over 18 hours, with a system weight over 700 tons.

Neutronics Considerations

Both the FBR and RBR are externally moderated cavity reactors. In order to make them as light weight and compact as possible, reflector thickness has been minimized. A 1-D neutron transport code (ANISN) calculates the size and critical mass of the two reactors. Limited 2-D neutron transport analyses, (DOT Code) have evaluated axial, power profiles and end effects for the RBR.

Fifteen neutron energy groups are used, of which seven are thermal. Cross sections were generated from ENDF/B data using the computer code NJOY. Table 4 illustrates some of the 1-D neutronic results for the RBR. For the RBR, 20% excess reactivity is assumed to account for neutron streaming out the nozzle, fuel burning, and reactor control.

Case one to three show how reflector thickness affect criticality. Less than 20 cm of reflecting material results in excessive neutron

leakage, while slowing down is essentially complete for reflectors beyond 30 cm of reflector thickness. Beryllium is the material of choice in the reactor design as its thermal diffusion length is large compared to its size.

Cases four to six illustrate the relationship between fissile fuel loading (note, highly enriched ^{235}U is used for all FBR and RBR designs), and k_{eff} . Above 67 kg there is only a small incremental gain in criticality per kg of U. Cases seven through nine show the effect of fluidized bed thickness over the limits of operation. As k_{eff} does not vary, with fluidization fluctuations in coolant flow or bed fluidization level do not pose a control problem. Cases ten through twelve examine the effect of the frit on criticality. Increasing the density of the frit is roughly equivalent to increasing its thickness or its absorption cross section. It is clear that frit absorption can have substantial effect on criticality. Cases thirteen and fourteen illustrate that H_2 pressure fluctuations will not significantly impact criticality. The density of H_2 atoms in the coolant gas is small compared with material at solid density so that fluctuations in coolant pressure do not significantly impact upon criticality. Helium has no measurable effect on criticality.

Table 5 presents selected 1-D neutronic calculations for the FBR. Ten percent excess reactivity is assumed to account for end losses and control. Cases one through four show the effect of fuel loading on criticality for a small reactor with a thin reflector. Note that even with a thin outer reflector, the fuel requirement is significantly below that of the RBR. Cases five through seven use a zirconium hydride outer moderator. Zirconium hydride does not perform well due to the excess capture neutrons in the outer zone. Zirconium deuteride is better, but Be remains the material of choice. Cases eight through ten demonstrate the effect of reflector thickness on criticality. Decreased fuel loading in the case of the FBR is due to the presence of the internal moderator. Cases eleven through thirteen show the effect of reflector thickness for a larger diameter higher power FBR.

In general, both the RBR and FBR can provide adequate excess reactivity in a compact design with minimal fuel loading. Both reactors are insensitive to variations in coolant flow and have temperature coefficients near zero.

Safety Considerations

Of prime concern are launch and reentry when considering space power reactor safety.

Launch phase safety requires not launching fission products. The reactor launch would be separate from the fuel loading (with the reactor subsequently loaded in space) or else with a large loading of a neutron poison (e.g., B_{4}C) in the core cavity. In either case, the reactor would be clean at launch.

The two most serious events identified to date are a launch failure leading to an ocean landing and burning up upon reentry with a radioactive core. In the event of an ocean landing, it is essential that the reactor package be designed so that criticality cannot occur. A reentry with a large fission product inventory is very unattractive. By carrying out acceptance testing at LEO and then transferring to an orbit high enough to have an orbit decay time greater than 300 years, fission products will have decayed to negligible levels before reentry could ever occur.

Total fissile and total transuranic inventories should be minimized. A smaller fissile inventory leads to less chance of launch hazard. As transuranics have a much lower MPC (Maximum Permissible Concentration) than uranium, using fully-enriched ^{235}U fuel virtually eliminates the risk associated with transuranic inventory.

The FBR/RBR are very simple and relatively inexpensive, it may be attractive to place spent space reactors in high orbits to decay following the unit's useful lifetime. Thus, the waste disposal problem is greatly simplified.

Conclusions

Space power systems based upon the RBR and FBR offer very high power levels at weights consistent with throw weight capabilities of presently available launch vehicles. Multi-megawatt power sources in space can be safe, reliable, and compact. The RBR and FBR would be inexpensive as well, due to their use of a developed fuel and the inherent simplicity of the designs. Any high-powered space reactor operating in a continuous, closed-cycle mode must reject large amounts of power to space radiatively. Careful design of such radiators is essential to any light-weight space power plant. By increasing the minimum operating temperature radiative heat transfer is enhanced, at the expense of thermodynamic efficiency. Using LDR's optimal designs are found which exhibit reasonably high thermal efficiencies due to the low specific weight of such radiators.

Within the 10- to 20- year time frame, such power stations as those described in this paper could be beaming power to earth and providing power to sustain life and perform a range of other tasks in space.

References

1. Binsley, R.L., High power study-turbine drive systems, Volume I: Analytical program, AFAPL-TR-10, Vol. II, Rockwell International, Rocketdyne Division, May 1976.
2. Tignac, L.L., High power study-turbine drive systems, Vol. II: AFAPL-TR-76-10, Vol. II, Rockwell International, Rocketdyne Division, May 1976.
3. Hodson, D.R., High power fast start turbine power unit, AFAPL-TR-78-34, Rocketdyne Division, Rockwell International, March 1978.
4. Schipper, L., High-power study—conventional generators, superconducting generators, non-air-breathing turbines, AFAPL-TR-76-39, Airessearch Manufacturing Co. of CA., a Division of the Garrett Corp., July 1976.
5. Southall, H.L. and Brockhurst, F.L., Permanent magnet and superconducting generators in air-borne, high-power systems, AFAPL-TR-79-2073, August, 1979.
6. Swift, H.F., Rejection of heat from space vehicles, International Applied Physics, Inc., IAP-TR-80-005, January 1980.
7. Powell, J.R., Botts, T.E., and Hertzberg, A., Applications of power beaming from space-based nuclear power stations, in Proc. 16th IECEC, Atlanta, GA., August 1981 (in press).

TABLE 1

Power Conversion Cycle Efficiencies (%) for
Turbine Brayton Cycle

| Reject temperature (K) | 500 | 700 | 900 |
|--------------------------------|------|------|-----|
| Reactor outlet temperature (K) | | | |
| 1000 | 6.4 | — | — |
| 1250 | 13.3 | 3.5 | — |
| 1500 | 19.4 | 8.5 | 2.0 |
| 1750 | 24.4 | 13.3 | 5.7 |

Nonregenerative Brayton
Cycle ($\eta_T = 0.85$, $\eta_c = 0.85$).

| Reactor outlet temperature (K) | 1000 | 1250 | 1500 | 1750 |
|--------------------------------|------|------|------|------|
| | 16.3 | 0.4 | — | — |
| | 26.7 | 10.7 | — | — |
| | 34.2 | 19.6 | 7.2 | — |
| | 40.0 | 26.7 | 15.0 | — |

Regenerative Brayton
Cycle ($\eta_T = 0.85$, $\eta_c = 0.85$, $\epsilon_R = 0.8$).

TABLE 2

Point Designs for Two MHD Channels for
Space Power Conversion

| | | |
|-----------------------|-----------|-----------|
| T coolant (exit) | 2500 K | 3000 K |
| Electrode hookup | diagonal | diagonal |
| Output power | 100 MW(e) | 100 MW(e) |
| Mass flow | 15.9 kg/s | 10 kg/s |
| P coolant (exit) | 100 bar | 100 bar |
| Generator inlet: | | |
| - stagnation pressure | 5.5 bar | 15 bar |
| - Mach No. | 0.84 | 1.4 |
| - width and height | 0.40 m | 0.2 m |
| Generator outlet: | | |
| - stagnation pressure | 1.035 bar | 1.76 bar |
| - Mach No. | 0.65 | 1.04 |
| - width and height | 0.84 m | 0.57 m |
| - half parameter | 4 | 4 |
| Length | 8.5 m | 6.2 m |
| Magnetic field | tapered | tapered |
| | 6 to 3 T | 6 to 3 T |
| Enthalpy extraction | 15% | 20% |

TABLE 3

Component Weights in Tons as a Function of Reactor Thermal Power In Megawatts

| Component | Weight as a function of reactor thermal power | $P_{in, MW(th)}$ |
|------------------------------------|---|------------------|
| Turbine | $3.5 \times 10^{-2} + 24.0 \times P$ | |
| Compressor | $5.0 \times 10^{-2} + 34.6 \times P$ | |
| Recuperator | $0.98 \times P$ | |
| Permanent magnet generator | $0.1 \times P$ | |
| MHD generator* | $25.0 \times P$ | |
| Piping | | |
| FBR ($P \leq 100 \text{ MW(e)}$) | $1.25 + 1.75 \times 10^{-2} \times P$ | |
| RBR ($P > 100 \text{ MW(e)}$) | $3.3 + 7.0 \times 10^{-4} \times P$ | |
| dc-dc convertor | 0.06 P | |
| Liquid Droplet Radiator | $1.44 \times 10^{11} \times P_{rej} T_{rej}^{-4}$ | |
| High-performance tube radiator | $9.7 \times 10^9 \times P_{rej} T_{rej}^{-4}$ | |

* Includes channel, diffuser, magnet, coolant, nozzle, and thermal shielding.

TABLE 4

One-dimensional Neutronic Analysis of the RBR
(Note, some cases are redundantly represented to facilitate comparison.)

| Case | Fuel Loading (kg 235U) | Cavity Thickness | Fuel Bed Thickness | Frit, ρ/ρ_0 | Reflector Thickness (cm) | H_2 Pressure, p/p_0 | k_{eff} |
|------|------------------------|------------------|--------------------|---------------------|--------------------------|-------------------------|-----------|
| 1 | 67 | 22 | 8 | 1 | 30 | 1 | 1.28 |
| 2 | 67 | 22 | 8 | 1 | 20 | 1 | 1.16 |
| 3 | 67 | 22 | 8 | 1 | 10 | 1 | 0.85 |
| 4 | 40 | 22 | 8 | 1 | 20 | 1 | 1.07 |
| 5 | 67 | 22 | 8 | 1 | 20 | 1 | 1.16 |
| 6 | 90 | 22 | 8 | 1 | 20 | 1 | 1.20 |
| 7 | 40 | 22 | 8 | 1 | 30 | 1 | 1.23 |
| 8 | 40 | 25.4 | 4.6 | 1 | 30 | 1 | 1.23 |
| 9 | 40 | 18.5 | 11.5 | 1 | 30 | 1 | 1.23 |
| 10 | 67 | 22 | 8 | 0 | 30 | 1 | 1.31 |
| 11 | 67 | 22 | 8 | 2 | 30 | 1 | 1.24 |
| 12 | 67 | 22 | 8 | 4 | 30 | 1 | 1.19 |
| 13 | 67 | 22 | 8 | 1 | 30 | .5 | 1.27 |
| 14 | 67 | 22 | 8 | 1 | 30 | 2 | 1.29 |

TABLE 5

One-dimensional Neutronic Analysis for the FBR
(Note: for cases one through ten, $\Delta R_2=2.0 \text{ cm}$, $\Delta R_3=1 \text{ cm}$ of Zr, $\Delta R_4=6.0 \text{ cm}$ with a 0.65 packing factor, $\Delta R_5=0.5 \text{ cm}$ of Zr, and $\Delta R_6=1.5 \text{ cm}$, and for cases eleven through thirteen, $\Delta R_2=4.0 \text{ cm}$ and $\Delta R_5=3.0 \text{ cm}$.)

| Case | Inner Moderator Material, ΔR_1 , cm | Outer Moderator Material, ΔR_7 , cm | Fuel Loading (kg) | k_{eff} |
|------|---|---|------------------------|-----------|
| 1 | C/16.0 | 10 | Be/15 | 1.01 |
| 2 | C/16.0 | 20 | Be/15 | 1.07 |
| 3 | C/16.0 | 35 | Be/15 | 1.12 |
| 4 | C/16.0 | 50 | Be/15 | 1.17 |
| 5 | C/16.0 | 20 | ZrH _{1.8} /15 | 0.85 |
| 6 | C/16.0 | 35 | ZrH _{1.8} /15 | 0.90 |
| 7 | C/16.0 | 50 | ZrH _{1.8} /15 | 0.94 |
| 8 | C/16.0 | 20 | Be/15 | 1.07 |
| 9 | C/16.0 | 20 | Be/20 | 1.21 |
| 10 | C/16.0 | 20 | Be/30 | 1.36 |
| 11 | C/26.5 | 20 | Be/15 | 1.13 |
| 12 | C/26.5 | 20 | Be/20 | 1.27 |
| 13 | C/26.5 | 20 | Be/30 | 1.41 |

TABLE 6

Variation of Specific Output Power as a Function of Output Power for a Closed-Cycle RBR/FBR Power Station

| Output Power Level (ME(e)) | Specific Power (ME(e)/MT) |
|----------------------------|---------------------------|
| 0.1 | .05 |
| 1.0 | .61 |
| 10.0 | 3.70 |
| 100.0 | 7.80 |
| 1000.0 | 8.35 |

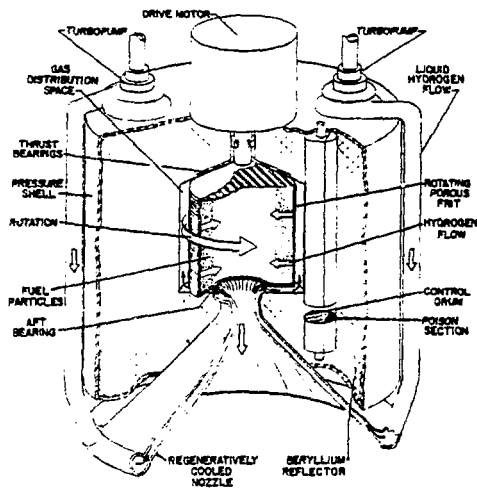


Figure 1

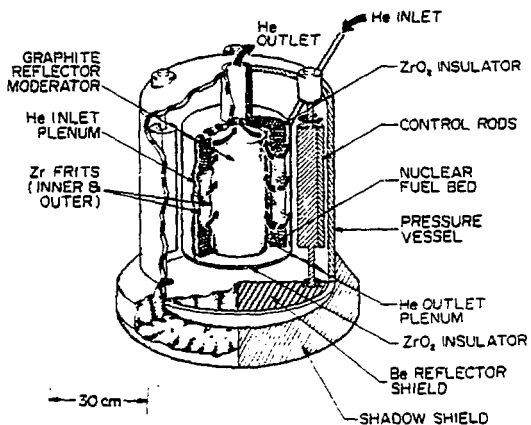
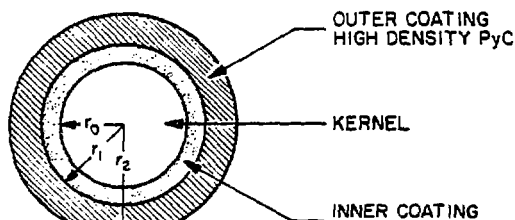
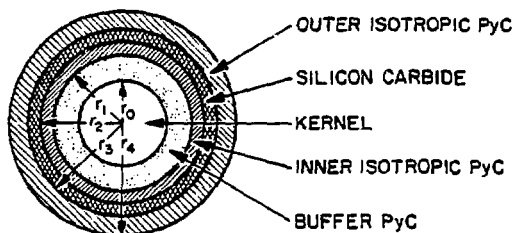


Figure 3



(a)



(b)

Figure 2

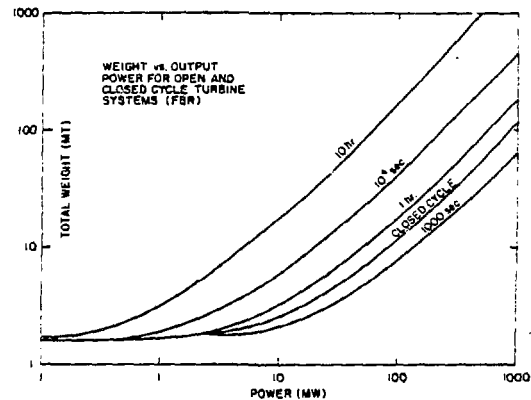


Figure 4

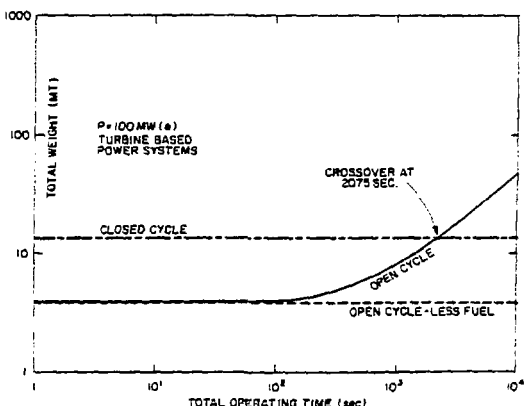


Figure 5